

Scaling of entanglement in finite arrays of exchange-coupled quantum dots

Jiaxiang Wang and Sabre Kais
Chemistry Department, Purdue University, West Lafayette, IN 47907

We present a finite-size scaling analysis of the entanglement in a two-dimensional arrays of quantum dots modeled by the Hubbard Hamiltonian on a triangular lattice. Using multistage block renormalization group approach, we have found that there is an abrupt jump of the entanglement when a first-order quantum phase transition occurs. At the critical point, the entanglement is constant, independent of the block size.

PACS numbers: 03.65.Ud,71.10.Fd,05.10.Cc

I. INTRODUCTION

After the pioneering work of Benioff [1], Feynman[2], and Deutsch [3] in field of quantum information and computing, the development in this field has been explosive in the past few years [4, 5]. A lot of exciting progresses have been made, such as the experimental realization of Shor's quantum factoring algorithm with NMR scheme for quantum computation [6], teleportation [7], cryptography [8] and dense coding [9]. Central to all these remarkable achievements is the concept of the quantum entanglements [10, 11, 12, 13, 14]. Just like energy, the entanglement has now been regarded as a controllable and a fungible physical resource [15]. Almost all the efficient protocols in quantum computing applications are based upon its generation. Experimentally, entanglements have already been produced among up to four photons [16, 17] and even between two macroscopic states such as two superconducting qubits, each of which contains as large as 10^9 electrons [18]. But theoretically, because an ensemble's Hilbert space grows exponentially with the number of its component particles, we are still far from fully understanding the contents of the entanglements. Only for the simplest state with two distinguishable particles can we have a complete description of the entanglement measure. For states of more than two particles, especially for mixed states, the current knowledge about their entanglement is very limited and all the related complexities have just begun to be explored.

II. ENTANGLEMENT MEASURE FOR FERMIONS

For spin-only entanglement of localized distinguishable particles, the most suitable and famous measure of the entanglement is the Wootters' measure [19]. Recently, Schlieman[20, 21] examined the influence of quantum statistics upon the definition of the entanglement. He discussed a two-fermion system with the Slater decomposition instead of Schmit decomposition for the entanglement measure. If we take each of the indistinguishable fermions to be in the single-particle Hilbert space C^N with f_m, f_m^+ ($m = 1, \dots, N$) denotes the fermionic annihilation and creation operator of single-particle states and $|\Omega\rangle$ represents the vacuum state. Then a pure two-electron state can be written as $\sum_{m,n} \omega_{mn} f_m^+ f_n^+ |\Omega\rangle$, where $\omega_{mn} = -\omega_{nm}$. In analogy to the Schmidt decomposition, it can be proved that every $|\Psi\rangle$ can be represented in a appropriately chosen basis in C^N in a form of Slater decomposition [20],

$$|\Psi\rangle = \frac{1}{\sqrt{\sum_{i=1}^K |z_i|^2}} \sum_{i=1}^K z_i f_{a_1(i)}^+ f_{a_2(i)}^+ |\Omega\rangle, \quad (1)$$

where $f_{a_1(i)}^+ |\Omega\rangle, f_{a_2(i)}^+ |\Omega\rangle, i = 1, \dots, K$, form an orthonormal basis in C^N . The number of the nonvanishing coefficients z_i is called the Slater rank, which is then used for the entanglement measure. With similar technique, the case of two-boson system is studied by Li [22] and Paškauskas [23].

Gittings [24] put forward three desirable properties of any entanglement measure: (a) Invariance under local unitary transformations; (b) Non invariance under non-local unitary transformations; (c) Correct behavior as distinguishability of the subsystems is lost. These requirements make the distinction between one-particle unitary transformation and one-site unitary transformations become relevant. As claimed in Ref. [24], a natural way achieving this distinction is to use a basis based upon sites rather on particles. Through Gittings' investigation, it is shown that all the above-discussed entanglement measures fail the tests of the three criteria. Only the Zanardi's measure [25] survives, which is given in Fock space as the von Neuman entropy, namely,

$$E_j = -Tr \rho_j \ln \rho_j, \rho_j = Tr_j |\psi\rangle \langle \psi|, \quad (2)$$

where Tr_j denotes the trace over all but the j th site and ψ is the antisymmetric wave function of the studied system. Hence E_j actually describes the entanglement of the j th site with the remaining sites. This measure is well operational numerically and will be used in our lattice systems, which uses the basis based upon sites from the start. A generalization of this one-site entanglement is to define an entanglement between one L-site block with the rest of the systems [29],

$$E_L = -Tr(\rho_L \log_2 \rho_L). \quad (3)$$

In this paper, this idea will be pursued together with the real-space renormalization group (RG) method.

III. ENTANGLEMENT AND QUANTUM PHASE TRANSITION

Quantum phase transition (QPT) is a qualitative change of some physical properties in a quantum many-body system as some parameter in the Hamiltonian is varied [26]. At the critical point when QPT happens, a long-range correlation can develop in the system. QPT is caused by quantum fluctuations at the absolute zero of temperature and is a pure quantum effect. Similarly entanglement is also a unique quantum property with non-local states of two or more quantum systems superposed with each other. Hence it is inviting to study the relationship between them. Recently it has been argued that the property responsible for the long-range correlation in QPT is entanglement [27]. So far, there have been some efforts in this direction, such as the analysis of the XY model about the single-spin entropies and two-spin quantum correlations [28], the entanglement between a block of L contiguous sites and the rest of the chain [29] and also the scaling of entanglement near QPT [30]. But because there is still no analytical proof to validate the above speculation, the role played by the entanglement in quantum critical phenomena remains elusive. Generally speaking, there are existing at least two difficulties in resolving this issue. First, until now, only two-particle entanglement is well explored. How to quantify the multi-particle entanglement is not clear. Second, QPT closely relates to the notorious many-body problems, which is almost intractable analytically except in some special toy models, such as the Ising model and the XY model. Until now, the only effective and accurate way to deal with QPT in critical region is the density-matrix RG method [32]. Unfortunately, it is only efficient for one-dimensional cases because of the much more complicated boundary conditions for two-dimensional situation.

In order to investigate the entanglement behavior in QPT for two-dimensional cases, we used the original real-space RG technique [31]. This method contains uncontrollable approximations. But by using bigger block size while at the same time comparing some of the obtained results with those already known from other methods to check the errors, we can still get reliable conclusions. For the entanglement measure, we used the Zanardie's measure. It is in essence a bipartite measure, but since most of the present quantum computation applications are concerning two-particle entanglement, it is still very meaningful and informative to carry out the study with it.

IV. CALCULATION METHOD

We have shown previously that for a half-filled triangular quantum lattice, there exists a metal-insulator phase transition with the ratio of electron repulsion and hopping term to be the tuning parameter [33, 34, 35]. In the following, we will use the same model and technique to explore the scaling properties of the entanglements.

The model we use is the Hubbard model with the Hamiltonian,

$$H = -t \sum_{\langle i,j \rangle, \sigma} [c_{i\sigma}^{\dagger} c_{j\sigma} + H.c.] + U \sum_i \left(\frac{1}{2} - n_{i\uparrow} \right) \left(\frac{1}{2} - n_{i\downarrow} \right) + K \sum_i I_i \quad (4)$$

where t is the nearest-neighbor hopping term, U is the local repulsive interaction and $K = -U/4$ and I_i is the unit operator. $c_{i\sigma}^{\dagger} (c_{i\sigma})$ creates(annihilates) an electron with spin σ in a Wannier orbital located at site i ; the corresponding number operator is $n_{i\sigma} = c_{i\sigma}^{\dagger} c_{i\sigma}$ and $\langle \rangle$ denotes the nearest-neighbor pairs. H.c. denotes the Hermitian conjugate. The order parameter for metal-insulator transition(MIT) is the charge gap defined by $\Delta_g = E(N_e - 1) + E(N_e + 1) - 2E(N_e)$, where $E(N_e)$ denotes the lowest energy for a N_e -electron system. In our case, N_e is equal to the site number N_s of the lattice. We already know that at the critical point $(U/t)_c = 12.5$, there will be a quantum phase transition, i.e. MIT, signature by a jump of Δ_g from Zero to non-zero. Unlike the charge gap calculated from the energy levels, the Zanardi measure of the entanglement is defined upon the wave function corresponding to $E(N_e)$

instead, as show in Eq. (2). Before showing how to get the entanglement from RG method, let us first briefly review the multi-staged real-space RG method.

The essence of real-space RG method is to map the original Hamiltonian to a new Hamiltonian with much fewer freedoms which keeps the physical quantities we are interested in unchanged [31]. The map can be iterated until the final Hamiltonian can be easily handled. The crucial step in this method is how to related the parameters between the old and the new Hamiltonians. This can be realized by dividing the original lattice into blocks and then build the new Hamiltonian upon blocks, namely regard each block to be an effective site.

Fig.1 shows schematically the hexagonal block structure we used in our calculations and the coupling between blocks. For each block, we solve it numerically in the subspaces of 6 electrons with 3 spin up and 3 spin down, 7 electrons with 4 spin up and 3 spin down, 7 electrons with 3 spin up and 4 spin down, and 8 electrons with 4 spin up and 4 spin down. In all the subspaces, we keep the lowest-energy non-degenerate state, which is also required to belong to the same irreducible representations of C_{6v} symmetry group. It should be mentioned here that if there is degeneracy then one possible solution is to average over the degenerated states. The kept states will then be taken as the 4 states for an effective site, $|0\rangle'$, $|\uparrow\rangle'$, $|\downarrow\rangle'$, $|\uparrow\downarrow\rangle'$. If denoting the energies corresponding to the first two states by E_1, E_2 , after some intensive calculations, we can obtain the new Hamiltonian on the effective lattice, which has the same structure as the original Hamiltonian, i.e.,

$$H' = -t' \sum_{\langle i,j \rangle, \sigma} [c'_{i\sigma}{}^+ c'_{j\sigma} + H.c.] + U' \sum_i \left(\frac{1}{2} - n'_{i\uparrow} \right) \left(\frac{1}{2} - n'_{i\downarrow} \right) + K' \sum_i I_i, \quad (5)$$

where the prime ' denotes the operator action upon the block states and

$$t' = 3\lambda^2 t, \quad (6)$$

$$U' = 2(E_1 - E_3), \quad (7)$$

$$K' = (E_1 + E_3)/2. \quad (8)$$

with $\lambda = \langle -\sigma, \sigma'_p c'_{i(p)\sigma}{}^+ | p - \sigma \rangle'_p = \langle \sigma'_p c'_{i(p)\sigma}{}^+ | 0 \rangle'_p$, where σ denotes \uparrow or \downarrow . The above equations are the so-called RG flow equations. Usually, they are iterated until we get the fixed point. But besides the fixed points, we can get more if we keep track of the results from each RG iteration. For example, if we stop the RG flow at the first iteration, then obtained t' and U' will be parameters of an effective 7-site hexagonal block mapped from the original system of 7^2 sites. Because the hexagonal block Hamiltonian can be solved numerically, then the physical quantities we have interest for a system containing 49 sites can be obtained. In this way, we can study the system of the size $7^2, 7^3, 7^4, 7^5, 7^6, \dots$. This is the so-called multi-stage real-space RG method, which is well adapted to start the finite-size scaling analysis. For entanglement, because at the i th iteration, the effective site involves 7^i starting sites, what we are calculating by this procedure is equivalent to get the entanglement between the L -site block and the surrounding seven L -site blocks. As L increases with the RG flow, the scaling of the entanglement with L comes out readily.

V. RESULTS AND DISCUSSIONS

In Fig. 2 we show the results of the entanglement as a function of (U/t) for different system sizes. The crossing point in Fig.2(a) represents the critical value of U/t , which is shown to be $(U/t)_c = 12.5$. It is exactly equal to the critical value for metal-insulator transition (MIT) when the same order parameter U/t is used [33, 34, 35]. In Fig.2(b), with proper scaling, all the curves in Fig.2(a) collapse onto one curve, which can be expressed as

$$E_7 = f(qN^{\frac{1}{2}}) \quad (9)$$

where $q = U/t - (U/t)_c$ measures the deviation distance of the system away from the critical state. By the one-parameter scaling theory, near the phase transition point, E_7 can written as

$$E_7 = q^{y_E} f\left(\frac{L}{\xi}\right) \quad (10)$$

where $\xi = q^{-\nu}$ is the correlation length of the system w here the critical exponent ν . Hence,

$$E_7 = q^{y_E} f(Lq^\nu) = q^{y_E} f(N^{\frac{1}{2\nu}} q), \quad (11)$$

where we used $N = L^2$ for the two-dimensional systems. Now we can have,

$$y_E = 0, \nu = 1 \quad (12)$$

It is interesting to note that here we have acquired the same ν as in the study of MIT. This shows the great consistency of the results since the critical exponent ν is only dependent upon the inherent symmetry and dimension of the investigated system.

Another significance of the results lies in the finding that in the metal state, the system is highly entangled with $E_7 = 2$ while in the insulating state, the system is partly entangled with $E_7 = 1$. Because the reduced density matrix ρ_7 is four dimensional, the maximally entangled state can be written as

$$\rho_7 = \begin{pmatrix} \frac{1}{4} & & & \\ & \frac{1}{4} & & \\ & & \frac{1}{4} & \\ & & & \frac{1}{4} \end{pmatrix}, \quad (13)$$

in the basis $|0\rangle, |\uparrow\rangle, |\downarrow\rangle, |\uparrow\downarrow\rangle$. The related entanglement is $E_7 = -\sum_{i=1}^4 \frac{1}{4} \log_2 \frac{1}{4} = 2$. Unlike the metal state, in which the sites can have equal probability in any of the four basis states, the insulating states should be expected to have electrons showing less mobility. From the calculations, we know that in the insulating state,

$$\rho_7 = \begin{pmatrix} 0 & & & \\ & \frac{1}{2} & & \\ & & \frac{1}{2} & \\ & & & 0 \end{pmatrix}, \quad (14)$$

which means that the central site has equal probability to be in $|\uparrow\rangle, |\downarrow\rangle$ and no occupation in $|0\rangle, |\uparrow\downarrow\rangle$. This well coincides with the above expectations. The corresponding entanglement is then $E_7 = -\sum_{i=2}^3 \frac{1}{2} \log_2 \frac{1}{2} = 1$.

All the above discussions are confined to the entanglement between the central site and its surrounding sites. Because the central site is a very special site showing the highest symmetry in the block, one may wonder what can happen to the neighbor sites, for example, the entanglement between site 1 and the rest 6 sites. To answer this question, the same calculations are conducted and the results are presented in Fig.3. Following the same procedures as for site 7, we can get the transition point and the critical exponents. It is no surprise that the same values are obtained. The only difference is that in the metal state, the maximal entanglement is a little less than 2 and the minimal one is a little less than 1. This can be explained by the asymmetric position of site 1 in the block.

It should be mentioned that the calculated entanglement here has a corresponding critical exponent $y_E = 0$. This means that the entanglement is constant at the critical point over all sizes of the system, which can be well seen from Fig.2(a) and Fig.3(a) also. But it is not a constant over all values of U/t . There is an abrupt jump across the critical point as $L \rightarrow \infty$, which can be easily seen in Fig.2(b) and Fig.(3)b. If we divide the regime of the order parameter into non-critical regime and critical regime, the results can be summarized as follows. 1) In the non-critical regime, i.e. U/t is away from $(U/t)_c$, as L increases, the entanglement will saturate finally onto two different values depending upon the sign of $U/t - (U/t)_c$. 2) At the critical point, the entanglement is actually a constant independent of the size L . These properties are qualitatively different from the single-site entanglement discussed by Osborne [28], where the entanglement with Zanardi's measure increases from zero to the maximum at the critical point and then decreases again to zero as the order parameter γ for XY mode is tuned. The peculiar properties of the entanglement we have found here can be of potential interest to make an effective ideal entanglement "switch". For example, with seven blocks of quantum dots on triangular lattice, the entanglement among the blocks can be regulated as "0" or "1" almost immediately once the tuning parameter $\frac{U}{t}$ crosses the critical point 12.5. The switch errors will depend upon the size of the blocks. Since it has already been a well-developed technique to change $\frac{U}{t}$ for quantum dot lattice, the above scheme should be well workable. To remove the special confinement we have made upon the calculated entanglement, namely only the entanglement of site 1 and site 7 with the rest sites are considered, in the following, we will prove that what we are switching here is actually the average pairwise entanglement between the seven blocks.

Let E_{ij} denotes the entanglement between i th and j th site. Then the total two-site entanglement E_{tot} can be obtained, i.e.

$$\begin{aligned} E_{tot} &= \sum_{i=2}^7 E_{1i} + \sum_{i=3}^7 E_{2i} + \sum_{i=4}^7 E_{3i} \\ &\quad + \sum_{i=5}^7 E_{4i} + \sum_{i=6}^7 E_{5i} + E_{67}. \end{aligned} \quad (15)$$

From the symmetry of the sites, we know that

$$\begin{aligned} E_{ij} &= E_{ji}, \\ E_{13} &= E_{24} = E_{35} = E_{46}, E_{14} = E_{25} = E_{36}, \\ E_{17} &= E_{27} = E_{37} = E_{47} = E_{57} = E_{67}. \end{aligned} \quad (16)$$

By substituting the above equalities into Eq. (15), we have,

$$E_{tot} = 6E_{17} + 3(2E_{12} + 2E_{13} + E_{14}). \quad (17)$$

Because

$$E_7 = 7E_{17}, E_1 = 2E_{12} + 2E_{13} + E_{14} \quad (18)$$

We finally have $E_{tot} = 6E_7 + 3E_1$. The average 2-site entanglement is $E_{average} = \frac{E_{tot}}{7} = \frac{1}{7}(2E_7 + E_1)$. Because

$$\begin{aligned} E_7 &= f(qN^{\frac{1}{2}}), \\ E_1 &= g(qN^{\frac{1}{2}}), \end{aligned} \quad (19)$$

then we should have $E_{average} = h(qN^{0.5})$. This tells us that the average pairwise entanglement also has the properties shown in Fig.2 and Fig.3.

Until now, almost all the finite-scaling work about the entanglements are done in one-dimensional cases, such as Ising model with transverse magnetic field or XY model. And different scaling properties of the entanglement are found there. In [36], the one-dimensional Harper Hamiltonian is investigated. The average concurrence shows different scaling properties in the metal and insulating states. In [29], Vidal calculated the entanglement with Zanardi measure between a L -site block with all the rest spin chains using XY model. And at the critical point, the entanglement demonstrates a logarithm dependence over the size L . Similar results are also found by Osterloh [30] in the concurrence derivative over the order parameter λ . None of the above work has reported the switching properties of the entanglement scaling over size. Hence it seems that the dimension of the investigated systems seem to play an important role also in the entanglement scaling, just as expected from QPT viewpoint.

VI. SUMMARY

In summary, by using a multi-stage real-space renormalization group method, the scaling properties of the entanglement with the Zanardi's measure over the block size when QPT happens has been investigated in details. The critical exponent $\nu = 1$ has been found, which coincides well with our previous work in studying a quite different physical property, the charge gap. When the block size $L \rightarrow \infty$, the entanglement shows an abrupt change when the tuning parameter crosses the phase transition point. This property might be well applied to make an "entanglement switch".

Acknowledgments

We would like to acknowledge the financial support of the Office of Naval Research(N00014-97-2-0192)

-
- [1] P. Benioff, J. Stat. Phys. 563, 22 (1980); Phys. Rev. Lett. 48, 1581 (1982).
- [2] R. P. Feynman, Int. J. Theor. Phys. 21, 467 (1982).
- [3] D. Deutsch, Proc. R. Soc. A 400, 97 (1985); Proc. R. Soc. A 425, 73 (1989).
- [4] C. H. Bennett and D. P. DiVincenzo, Nature 404, 247 (2000).
- [5] C. Monroe, Nature 416, 238 (2002).
- [6] L. M. K. Vandersypen, M. Steffen, G. Breyta, C. S. Yannoni, M. H. Sherwood and I. L. Chuang, Nature 414, 883 (2001).
- [7] D. Bouwmeester, J. Pan, K. Mattle, M. Eibl, H. Weinfurter and A. Zeilinger, Nature 390, 575 (1997).
- [8] T. Jennewein, C. Simon, G. Weihs, H. Weinfurter and A. Zeilinger, Phys. Rev. Lett. 84, 4729 (2000).
- [9] K. Mattle, H. Weinfurter, P. G. Kwiat and A. Zeilinger, Phys. Rev. Lett. 76, 4546 (1996).
- [10] M. Lewenstein, D. Bruss; J. I. Cirac, B. Kraus, M. Ku, J. Samsonowicz, A. Sanpera and R. Tarrach, J. Mod. Opt. 47, 2841 (2000).
- [11] M. Horodecki, P. Horodecki, R. Horodecki, e-print, quant-ph/0109124.
- [12] M. J. Donald, Michal Horodecki, Oliver Rudolph, e-print, quant-ph/0105017.
- [13] B. M. Terhal, e-print, quant-ph/0101032.
- [14] D. Bruss, J. Math. Phys. 43, 4237 (2002).
- [15] M. A. Nielsen, C. M. Dawson, J. L. Dodd, A. Gilchrist, D. Mortimer, T. J. Osborne, M. J. Bremner, A. W. Harrow and A. Hines, Phys. Rev. A 67, 052301 (2003).
- [16] A. Lamas-Linares, J. C. Howell and D. Bouwmeester, Nature 412, 887 (2001).
- [17] M. Eibl, S. Gaertner, M. Bourennane, C. Kurtsiefer, M. Zukowski and H. Weinfurter, Phys. Rev. Lett. 90, 200403 (2003).
- [18] A. J. Berkley, H. Xu, R. C. Ramos, M. A. Gubrud, F. W. Strauch, P. R. Johnson, J. R. Anderson, A. J. Dragt, C. J. Lobb, F. C. Wellstood, Nature 300, 1548 (2003).
- [19] W. K. Wootters, Phys. Rev. Lett. 80, 2245 (1998).
- [20] J. Schliemann, J. Ignacio Cirac, M. Kus, M. Lewenstein and D. Loss, Phys. Rev. A 64, 022303 (2001).
- [21] J. Schliemann, D. Loss and A. H. MacDonald, e-print, cond-mat/0009083.
- [22] Y. S. Li, B. Zeng, X. S. Liu and G. L. Long, Phys. Rev. A 64, 054302 (2001).
- [23] R. Paškauskas and L. You, Phys. Rev. A 64, 042310 (2001).
- [24] J. R. Gittings and A. J. Fisher, Phys. Rev. A 66, 032305 (2002).
- [25] P. Zanardi, Phys. Rev. A 65, 042101 (2002).
- [26] S. Sachdev, *Quantum Phase Transitions* (Cambridge University Press, Cambridge, 1999).
- [27] T. J. Osborne and M. A. Nielsen, e-print, quant-ph/0109024.
- [28] T. J. Osborne and M. A. Nielsen, Phys. Rev. A 66, 032110 (2002).
- [29] G. Vidal, J. I. Latorre, E. Rico and A. Kitaev, e-print, quant-ph/0211074.
- [30] A. Osterloh, L. Amico, G. Falci and R. Fazio, Nature 416, 608 (2002).
- [31] *Real-Space Renormalization* (Topics in Current Physics), Editors: T. W. Burkhardt and J. M. J. van Leeuwen, Springer-Verlag, 1982.
- [32] S. R. White, Phys. Rev. Lett. 69, 2863 (1992).
- [33] J. X. Wang, S. Kais and R. D. Levine, Int. J. Mol. Sci. 3, 4 (2002).
- [34] J. X. Wang, S. Kais, Phys. Rev. B 66, 081101(R) (2002).
- [35] J. X. Wang, S. Kais, F. Remacle and R. D. Levine, J. Chem. Phys. B 106, 12847(2002).
- [36] A. Lakshminarayanan and V. Subrahmanyam, Phys. Rev. A 67, 052304 (2003).

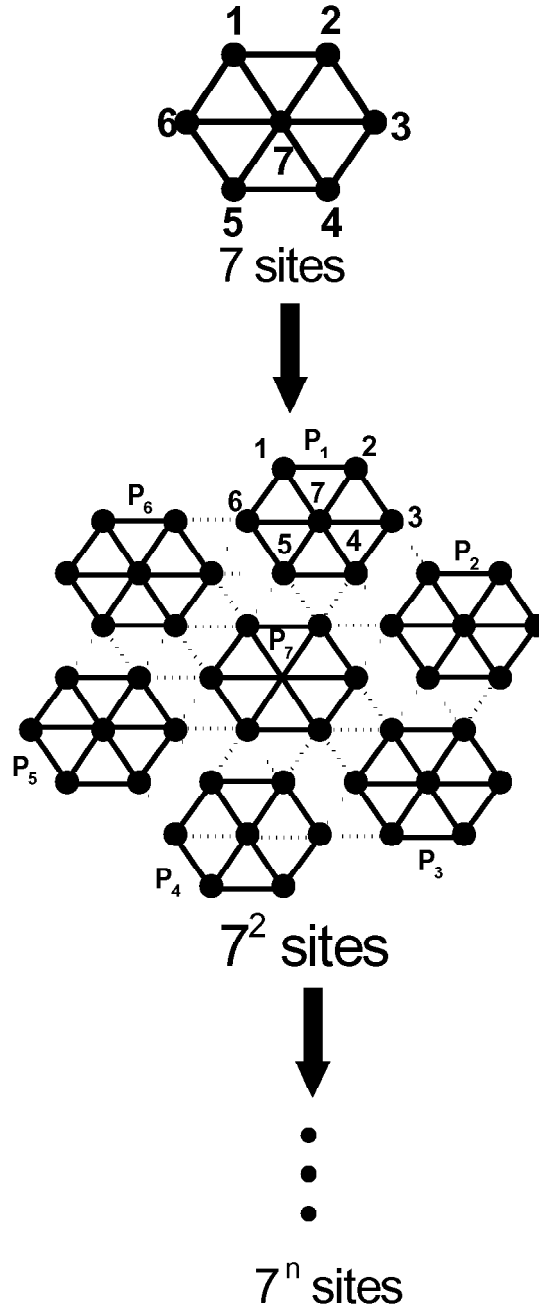


FIG. 1: Schematic diagram of the triangular lattice with hexagonal blocks. The hexagonal block is used for the renormalization process. The iteration direction is shown by the arrow. The dotted lines represent the interblock interactions and solid line intrablock ones.

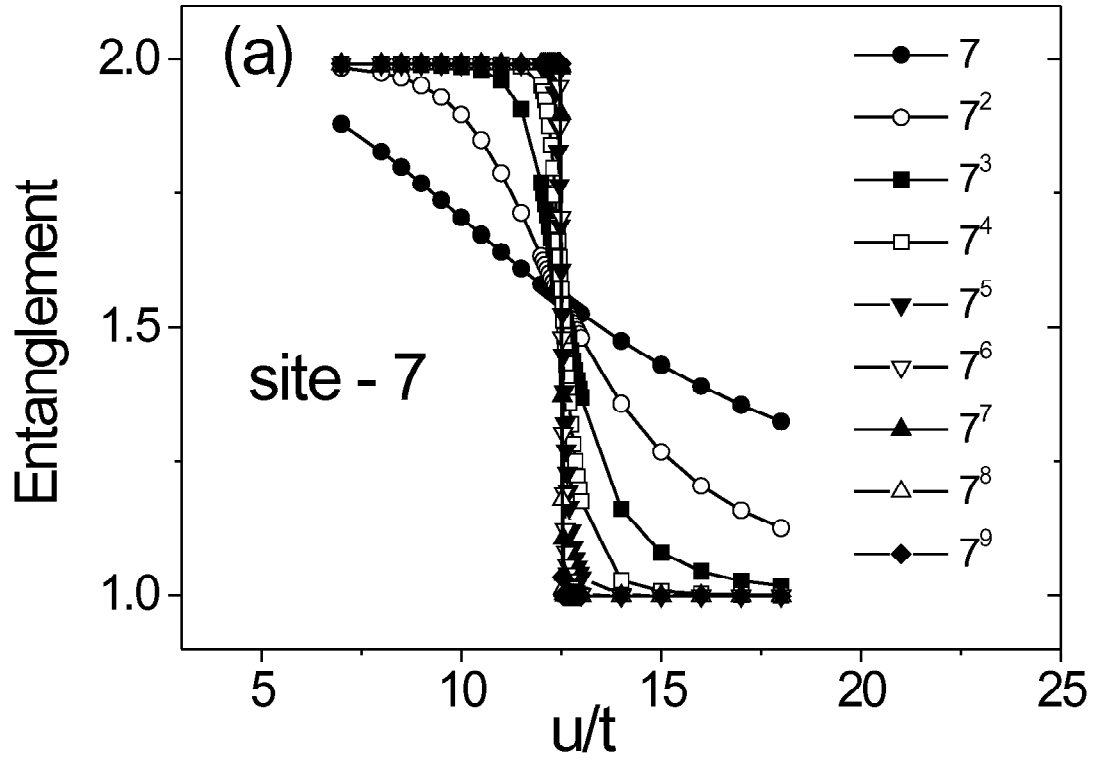


FIG. 2: Variations of the entanglement between site 7 and the neighboring sites (See Fig.1) against the ratio of on-site electron interaction U to the hopping term t for different system size, i.e. the number of sites: 7 (solid circle), 7^2 (open circle), 7^3 (solid square), 7^4 (open square), 7^5 (solid down triangle), 7^6 (open down triangle), 7^7 (solid up triangle), 7^8 (open up triangle), 7^9 (solid diamond)

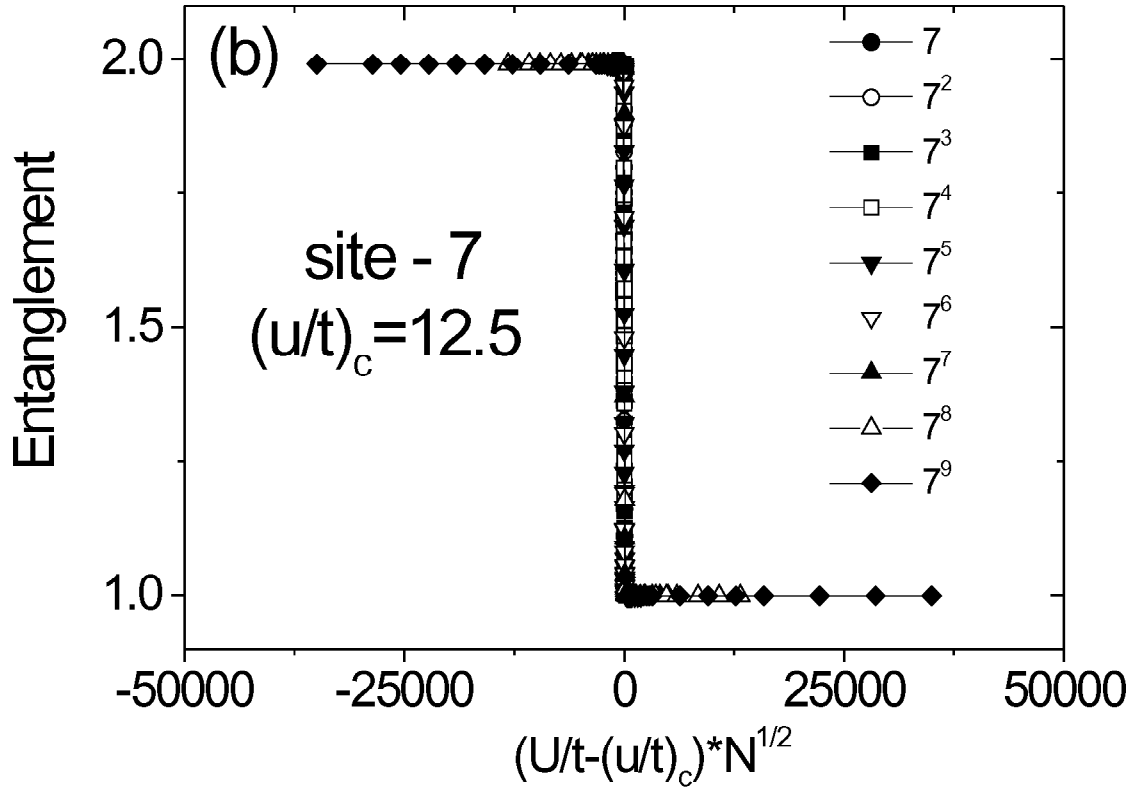


FIG. 3: Variations of the entanglement between site 7 and the neighboring sites (See Fig.1) against the ratio of on-site electron interaction U to the hopping term t for different system size, i.e. the number of sites: 7 (solid circle), 7^2 (open circle), 7^3 (solid square), 7^4 (open square), 7^5 (solid down triangle), 7^6 (open down triangle), 7^7 (solid up triangle), 7^8 (open up triangle), 7^9 (solid diamond)

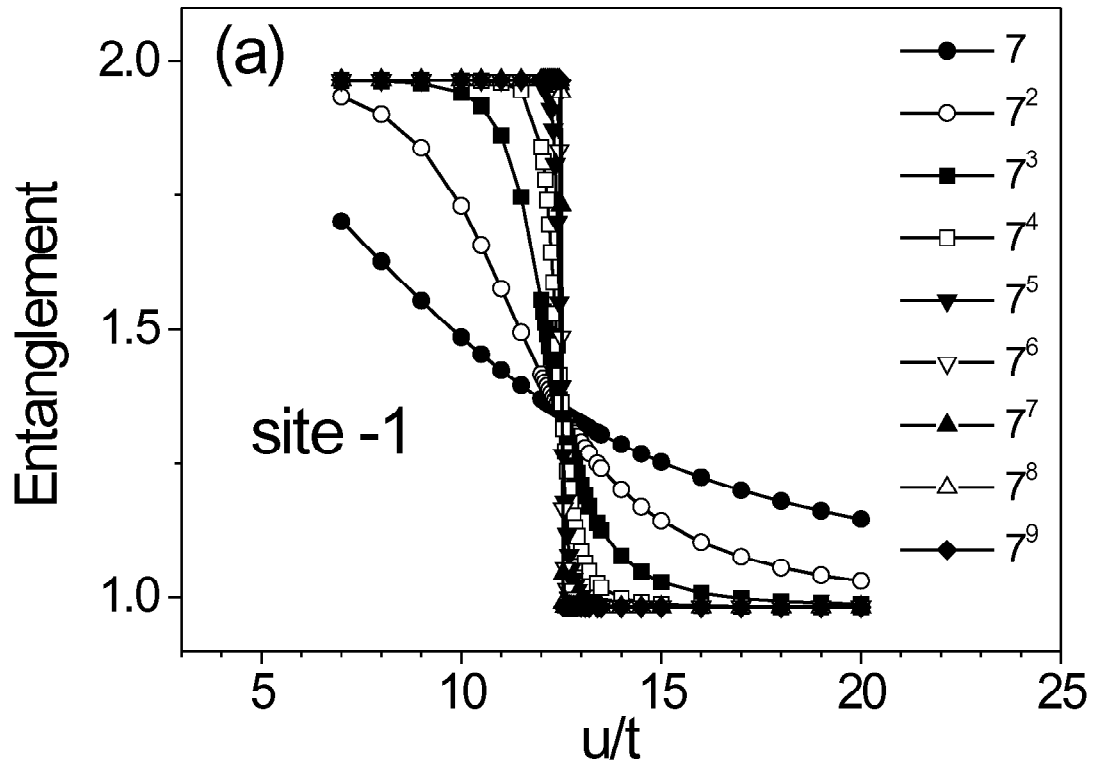


FIG. 4: The same as in Fig.2, but for the entanglement between site 1 and the rest 6 sites of the block.

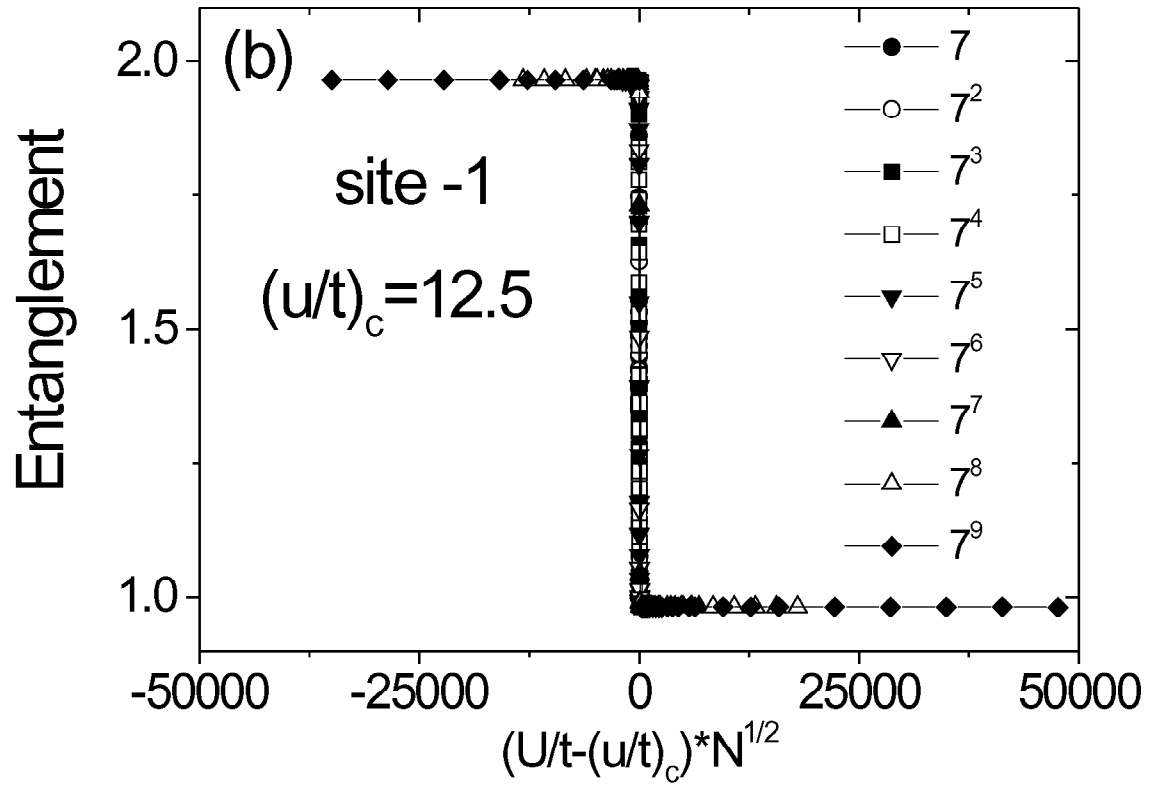


FIG. 5: The same as in Fig.2, but for the entanglement between site 1 and the rest 6 sites of the block.